Evaluating the Impact of Power Outages on Occupancy Patterns During the 2021 Texas Power Crisis

Andy Berres*
National Renewable Energy Laboratory

Baldwin Nsonga†
Leipzig University

Caitlyn Clark‡
National Renewable Energy Laboratory

Robert Jeffers§
National Renewable Energy Laboratory

Hans Hagen¶
University of Kaiserslautern-Landau

Gerik Scheuermann‖
Leipzig University

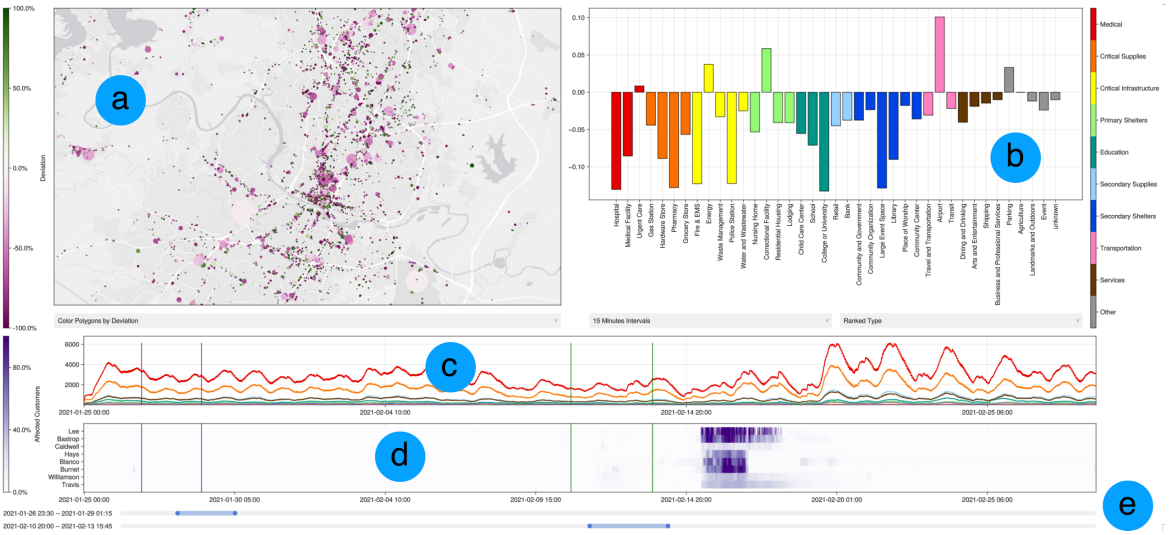

Figure 1: An overview of the MoVis analysis tool (cf. section 4). (a) shows the map with circles that indicate high mobility in specific locations. Users can zoom into the map to see building polygons and display additional information. (b) shows the deviation of movement patterns between two selected time ranges. The colors indicate the category associated with the deviation of a specific type. (c) shows the number of travels over time for each category (d) displays the temporal outage *severity* for previously selected counties relevant to the study. (e) shows sliders that allow the user to select time ranges for comparison. The selected ranges are shown in (c) and (d) as purple and green vertical line pairs.

Abstract

Large-scale power outages, such as those caused by extreme weather events, have a big impact on human behavior. A short power outage is merely a nuisance for most, and may not change people's locations. An outage that lasts for a few hours can result in spoiled food and medical supplies, and people will have to restock spoiled items. Long outages result in temperatures outside tolerable levels in homes, and may prompt people to acquire supplies, such as generators and gas, or change location. The long outages during Winter Storm Uri in Texas resulted in millions of dollars in property damage due to freezing pipes. This level of damage is expected to result in a sharp increase in supply runs and contractor activity.

In this paper, we present a tool to explore differences in visiting patterns before, during, and after power outages. It allows to compare different points of interest like medical facilities, grocery stores, hardware stores, and other types of businesses.

*e-mail: andy.berres@nrel.gov
†e-mail: nsonga@informatik.uni-leipzig.de
‡e-mail: caitlyn.clark@hq.doe.gov
§e-mail: bobby.jeffers@nrel.gov
¶e-mail: hagen@informatik.uni-kl.de
‖e-mail: scheuermann@informatik.uni-leipzig.de

Index Terms: Power outage, point of interest visits, geospatial.

1 Introduction

In February 2021, Winter Storm Uri made headlines when it caused widespread power outages in Texas, leaving about 10 million Texas residents without electricity, causing billions of dollars in economic damage and costing several dozen lives. The energy infrastructure, housing stock, and the general population were not prepared for the extreme temperatures caused by Uri, which were $22-28°C/40-50°F$ below average winter temperatures [9].

The extreme temperatures caused a dramatic decline in available energy [9] at a time of extremely high demand as households struggled to stay warm. Most of the Texas power grid is part of an electric interconnection that is isolated from the rest of the United States and Canada, making electricity trading with unaffected regions impossible. According to the Texas Department of State Health Services, hundreds of lives were lost during this energy crisis due to hypothermia, carbon monoxide poisoning due to inappropriate use of indoor generators, and the loss of power to critical medical equipment [27]. In many homes, frozen pipes caused immense damage to the property. 75% of Texans had difficulty obtaining food, as food in homes and grocery stores had spoiled [17].

Rather than studying the impact of the weather directly, the objective of this paper is to gain insight into the impact of the energy crisis on occupancy. In building energy research, occupancy is commonly used to determine the human impact on energy use [2, 1]. In case of the energy crisis, we want to understand the im-

pact of energy on humans by applying this metric in reverse. In this case, occupancy can serve as a measure of how many people are affected.

In this paper, we propose a tool to analyze changes in occupancy patterns at urban scale and evaluate the relationship between power outages and human behaviors at the example of the Texas winter storm outages. Using mobility data, we will study the population's visits at points of interest in Austin to better understand how residents responded to the energy crisis in preparation of the storm, during outages, and in the aftermath.

2 Related Work

Visual analytics approaches for urban data have been extensively studied, as shown in the surveys: [19, 11, 29]. In the context of visualizing data on maps, generalization, aggregation, and simplification were widely used to simplify building representations [25, 28, 10] or maps in general [15]. For 3D building data, occlusion also plays a major role. Hirono et al. [14] introduced a disoccluding technique for building data. In the context of mobility patterns in urban areas, various studies have been conducted [8, 16, 21, 13, 30, 31]. Most visualization schemes related to mobility focus on depicting heatmaps of values of interest. Alternatively, authors utilize graphs to encode an visualize different trips. Although a graph representation would be suitable for the depiction of mobility patterns and change, we want to keep the level of abstraction low and focus on an intuitive exploration of the data.

Previous work on the impact of power outages on humans has focused on studying disparities between different counties during Uri on an aggregate scale of total hours of consecutive outages [12], and assessing the overall burden of the household [23]. Both works were based on survey data and the focus was on an in-depth analysis of the findings. Another work studied the spatial distribution of power outages in relation to social vulnerability [7]. Although all three of these works study human behavior and impact during power outages, they are complementary to the goals of this work, as we evaluate externally visible impact in time series data while the surveys used in these studies inquired overall experiences, such as duration of the outage, difficulty acquiring food, and property damage.

3 Dataset

3.1 Point of Interest (POI) Visits

The POI visit data for Austin, Texas was purchased from Resilient Solutions 21 (RS21). These data use cellphone-based GPS data to determine individual device locations and map them to Foursquare POIs.The visit data contain: anonymous device ID, home location, visit start and end times, distance from home in meters, POI ID, and POI name. To protect privacy, the home location of each device is set to the Census home block group. A second file provides the POI ID and the geometry of the building (Microsoft building footprints [18]) for each building. A third file contains the mapping from POIs to buildings: POI name, address, lat/lon centroid, building ID, and building geometry [18]. Austin has 127,392 POIs in 52,553 buildings. The raw visit data consist of 2,477,95,413 rows for the interval from January 1 to March 31, 2021.

3.2 Customer Outages

To provide context for visit behaviors, we use power outage data from the Environment for Analysis of Geo-Located Energy Information (EAGLE-I) [26] platform. These are 15-minute county-level data, and each timestep includes the Federal Information Processing Standards (FIPS) code, state and county name, and number of customers without power. In addition, modeled total customer counts are available for each county [4, 20].

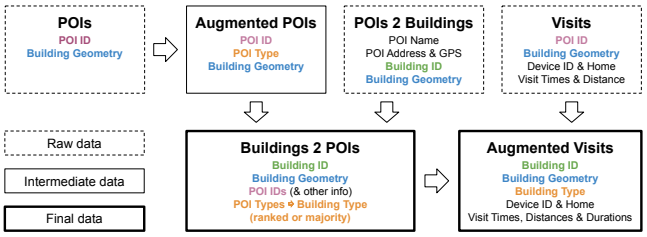

Figure 2: Data fusion steps from original data to the final visit data. The different steps are linked through POI IDs (pink font) and types (orange), building IDs (green), and building geometry (blue).

4 Methodology

The purpose of the proposed tool (MoVis) is to interactively compare mobility patterns between different time ranges. It should provide context, allowing the user to identify time regions of interest and investigate them in detail. Figure 1 provides an overview of the tool.

The application is written in Julia [3], and we chose the Makie framework [6] to create the interactive user interface and visualizations, as its support for OpenGL and WebGL makes it adaptable and scalable.

4.1 Preprocessing

Data Fusion Several data fusion steps of data fusion were needed to combine the different data products into a consolidated dataset (cf. Figure 2). First, we defined a mapping between POI IDs (pink) and building IDs (green) by joining the data based on the shared building geometry (blue). We furthermore added POI types (orange) to the POI data, and provided building types in three ways: a full dictionary of all POI types and their counts, a *majorityType* which is the most frequent POI type in a building, and a *rankedType* which chooses the POI type with the highest priority type present, using a manually created ranking. The legend for Figure 1b shows a ranking of POI type groups from most (top) to least (bottom) important.

Augmenting POI Type To better understand visit behavior, we are interested in what types of POIs people visit. As the raw POIs we received did not include classifications, we first performed a keyword-based mapping from business names to 39 different POI types (cf. Figure 1 (b)), using a set of 450 manually selected keywords that can reliably identify business types (e.g., "taco", "surgery", or names of big chains). This resulted in a successful classification of 81,073 POI types. For the remaining 46,318 POIs, we used gpt-4-turbo to perform a classification. In small increments of 50 POIs (to ensure that the model would return classifications rather than a generic response), we provided the list of possible classifications and a list of POI names, and requested a classification, confidence level, and rationale for the classification. Several hours of manual review and cleaning later, we were left with 2,315 unclassified POIs that were manually classified. Finally, we defined 10 coarse classification categories for visualization purposes.

Cleaning Visits When we began working with the visit data, we found extremely high rates of visits. Further investigation revealed that this issue was caused by buildings with multiple POIs as each POI has the geometry for the full building, the data counted a visit for each POI in these buildings at each time step. We aggregated these data by identifying the first and last consecutive timestamps during which a device visited a building and aggregating the other fields accordingly. This reduced the dataset size by 96.4% to 9,040,695 rows of visit data. During this cleaning step, we also appended visit durations to each row.

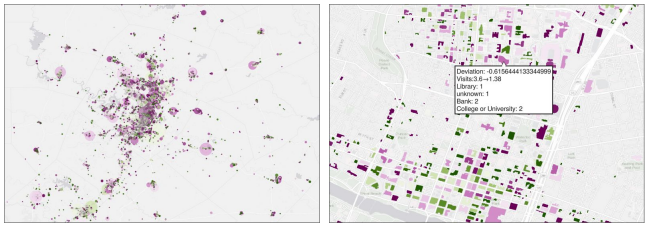

Figure 3: The map view visualizes travel activity using scatter plots when zoomed out (left), and switches to colored building polygons when zoomed in (right). Green indicates and increase in activity compared to the baseline, whereas magenta indicates a decrease. The mouseover of the university library building shows a 61% decrease in activity. The building's POI types include library, university, and bank (ATMs).

Binning For this work, we denote the number of visits as $v_b(t)$, where v is the number of visits to a building b at a time step t. The high temporal resolution of the visit times, provided with an accuracy in seconds, makes aggregating individual visits challenging. We found a binning approach to be adequate to aggregate visits that occur seconds apart. Here, we chose a temporal resolution of 15 minutes. In this processing step, we also filter out multiple visits by a single device in short time frames using the unique ID. Then aggregation is performed on the binned data, where t is a 15 minute multiple. Therefore, $v_b(t)$ describes the number of visits by unique devices in 15 minute intervals.

Performance The occupancy data introduced in the previous section is provided as a list of visits in temporal order. In terms of data management, this is not suitable for an interactive exploration of the time domain for individual locations. In this preprocessing step, we structure the data in a way that allows quick access to the outage data for a specific building at a specific time step by isolating the occupancy by building and storing only the time steps for which these data are available.

4.2 Map view

This view aims to visualize the occupancy information for the buildings. We display the buildings based on their outline polygon. Note that a building can include multiple points of interest. A dropdown list allows the user to color the polygons based on the deviation, the building *majorityType* or the building *rankedType*. The last two options visualize the building category directly with a coloring based on the preprocessed data and the chosen color scheme. The deviation is computed as follows. First, given a user-selected time range $r = (t_1, t_2)$, the average visits over a time range are calculated as follows:

$$\bar{v}_{(t_2,t_2)}(b) = \frac{1}{N}\sum_{t\in r} v_b(t), \tag{1}$$

where N is the amount of samples within the time range. With the default of 15 minutes between samples, the user can also select step sizes of 1 Hour, 24 Hours, or 7 days to account for periodic fluctuations in occupancy patterns. We define the deviation as:

$$d_{r_1,r_2}(b) = \frac{\bar{v}_{r_1}(b) - \bar{v}_{r_2}(b)}{\bar{v}_{max}(b)}, \tag{2}$$

where b is a building. The user can set the two time ranges r_1 and r_2 using range sliders (cf. Figure 1(e)). The deviation $d_{r_1,r_2}(b) \in \mathbb{R}$ ranges from -1 to 1 and encodes the relative change of occupancy. This normalized metric allows the user to investigate variations independently of the total number of visits, which could skew the visualization toward frequently visited locations. By default, the building polygons are colored according to the deviation $d_{r_1,r_2}(b)$. This allows a local investigation of the occupancy variation, whereas coloring by type allows for a quick overview of POIs in the area. Detailed information on a building is displayed when hovering the mouse cursor over the polygon.

When zooming out, the number of polygons in the view increases and individual polygons become hard to see. To counteract this, we enable the scatter plot view when a set threshold for the zoom level is reached (cf. Figure 3). This aims to provide an overview and help the user quickly identify regions of interest with high counts of visits and deviations. The scatter point locations correspond to the bounding box centers of the polygons. The size of the scatter points is based on $\bar{v}_{max}(b) = |max[\bar{v}_{r_1}(b), \bar{v}_{r_2}(b)]|$, where a larger point size is associated with locations with a high average visit value. The colors of the scatter plot are based on the deviation $d_{r_1,r_2}(b)$ analogous to the polygon view.

In addition to the polygons and scatter plot, we integrated tiled web maps to provide geographical context. While the deviation is shown using a divergent color map, the color scheme of the coarse categories was generated manually with nameability in mind [24].

4.3 Aggregate Deviation Chart

The purpose of this chart is to provide the user with an overview of deviations in visits for the entire area (cf. Figure 1(b)). For every building type n, we compute the normalized aggregate deviation as follows:

$$\bar{d_n}(r_1, r_2) = \frac{1}{|b \in n|}\sum_{b\in n} d_{r_1,r_2}(b) \tag{3}$$

The color scheme is based on the coarse categories analogous to the type coloration of the polygons. Note that the types n are more detailed than the coarse categories. The order of the types is based on the category ranks, where the types with the highest rank are on the left. As buildings can contain multiple POIs from different categories, the selection menu allows the user to choose between *rankedType* and *majorityType* for visualization.

4.4 Timeline

The timeline consists of two visualizations (cf. Figure 1(c,d), each highlighting the two intervals that are compared using purple (before) and green (after) vertical bars.

The top graph is a line graph that displays the overall visits over time separated by categories (cf. Figure 1(c)). The graph displayed reacts to the category selection option (*rankedType* or *majorityType*). For every category c we compute:

$$\hat{v}_b(c;t) = \sum_{b\in c} v_b(t), \tag{4}$$

The lower visualization displays outages over time in previously selected counties using a heatmap (cf. Figure 1(d)). We define the normalized outage value:

$$o(c;t) = \frac{\text{affected customers at time } t}{\text{modeled customer count at time } t}, \tag{5}$$

where c is a county and t is time. In some cases $o(c;t)$ can be larger than 1 as a result of the imprecision in the modeled customer counts. This visualization adds context to the analysis by providing an overview of the temporal dynamics of the power outage and helps the user identify potential time regions of interest.

5 Case Study

We demonstrate MoVis by comparing visits before, during, and after the Uri outages, and summarize the relevant visualizations in Figure 4. We chose three intervals of 72 hours: the time window of the highest outages, beginning on February 15 at 7:00 (purple (g)), two weeks before (gray) as a baseline, and one week later as

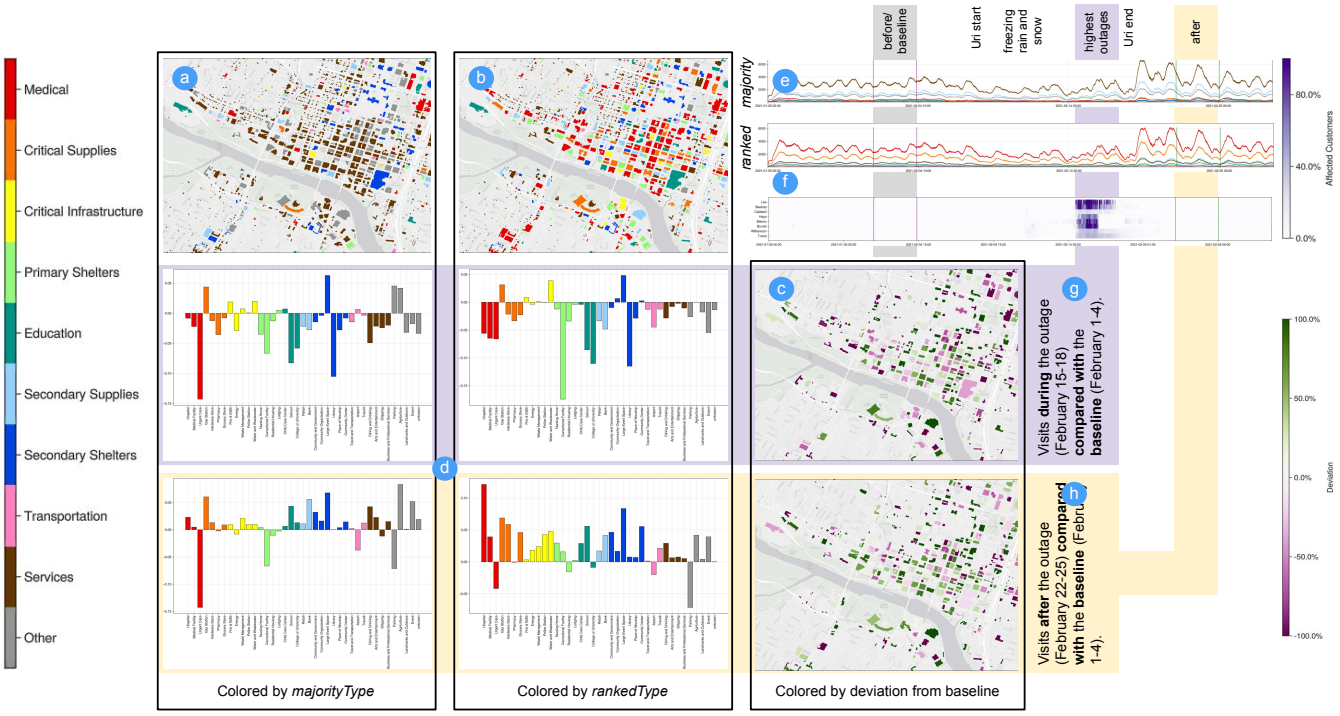

Figure 4: Collection of visualizations of visits during Winter Storm Uri. The vertical boxes show maps (a-c) and charts (d) using *majorityType* (left), *rankedType* (middle), and deviation from baseline (right) as building types for aggregation and rendering. The top right shows timeline views for both renderings (e), as well as power outages (f). Vertical boxes behind the timeline highlight the three chosen intervals: baseline (gray), during (purple), and aftermath (yellow). The same color is also used to indicate which time interval is compared with the baseline (g-h).

"after" (yellow (h)). The time frames are aligned to cover identical times and weekdays to account for similar behavioral time-of-day and weekday patterns. We compare two different UI selections that share the baseline time frame as the first time frame. One uses the outage for the second time frame (purple background), and the other uses the week after the main outages as the second time frame (yellow background).

During the outages, activities declined sharply for the majority of POI types compared to the baseline; however, some types saw an increase: gas stations (potentially to purchase fuel for generators), critical infrastructure such as emergency services and utilities, and large event spaces (which were used as cold shelters [5]). After the outages, activity increased across almost all POIs, compared to the baseline. The most notable increases are those of Hospital and Medical Facility visits, which may be due to adverse health conditions due to hypothermia, carbon monoxide poisoning, or ill effects from unsafe drinking water [27, 5]. Other notable increases include grocery stores (likely to replace spoiled food items), and hardware stores (likely to purchase supplies to repair home damage).

The timeline charts (e) show a clear pattern of daily activity for each POI type. In the week before the main outages, there was a visible decrease in activity across all types. During this period, the area experienced six inches of snow and one inch of solid ice from freezing rain.

The side-by-side comparison of building types (d) illustrates the difficulty of deciding how to classify a building containing multiple POIs. Hospitals usually have some food service options for visitors, and many large buildings have a wide variety of businesses (e.g. a building could have law firms, barbers, restaurants, a bank, and medical providers in different suites). Providing users with two options allows them to get different views of the data. We also explored providing a full set of POI types in the hover-over menu but found that it was too much content for multi-use buildings.

6 Conclusion

We proposed a tool to interact and explore occupancy data in the context of a severe power outage. The tool focuses on comparing occupancy patterns between different time intervals that the user selects. Changes in occupancy patterns can be explored using the sliders to define and move the time intervals.The deviation provides an easy-to-interpret metric for changes in the occupancy, and its analysis can be performed to investigate categories changes or local changes in the urban environment. The presented case study highlights the usefulness of the presented tool.

We plan to extend the tool to represent the temporal evolution of visits and will evaluate ways to provide a more intuitive visualization of multiple POI types within the buildings. With regard to the map view, it would be appropriate to investigate different abstractions of the buildings to encode information while respecting the geographic context. In addition, we want to visualize the uncertainty of the geographic location of devices in relation to POIs.

We plan to integrate a more detailed analysis of power outages in relation to weather [22]. Furthermore, we plan to integrate distance from home, visits at similar POIs to attempt to reproduce Peterson et al.'s [23] finding that some people experienced difficulty in acquiring food during the winter storm. We also want to include changes in visit duration as an increase may indicate busier stores (higher store occupancy), more required shopping to restock goods, or trouble finding alternatives to out-of-stock items. Finally, we plan to evaluate equity by incorporating block-group-level Census data to compare behaviors of different demographic groups before/during/after outages. Differences could indicate less access to electricity (longer/more frequent outages), backup power, and energy storage; or non-energy factors such as less stockpiled food, or insufficient heating for human comfort and safety, which could be indicated by visits to cold shelters.

Acknowledgments

This work was authored in part by the National Renewable Energy Laboratory, operated by Alliance for Sustainable Energy, LLC, for the U.S. Department of Energy (DOE) under Contract No. DE-AC36-08GO28308. Funding was provided by Laboratory Directed Research and Development funds. The views expressed in the article do not necessarily represent the views of the DOE or the U.S. Government. The U.S. Government retains and the publisher, by accepting the article for publication, acknowledges that the U.S. Government retains a nonexclusive, paid-up, irrevocable, worldwide license to publish or reproduce the published form of this work, or allow others to do so, for U.S. Government purposes.

This work was partially funded by the German Federal Ministry of Education and Research within the project Competence Center for Scalable Data Services and Solutions (ScaDS) Dresden/Leipzig (BMBF 01IS14014B).

A portion of the research was performed using computational resources sponsored by the Department of Energy's Office of Energy Efficiency and Renewable Energy and located at the National Renewable Energy Laboratory.

Support for power outage dataset is provided by the U.S. Department of Energy, project EAGLE-I under Contract 31256. Project EAGLE-I used resources of the Oak Ridge Leadership Computing Facility at Oak Ridge National Laboratory, which is supported by the Office of Science of the U.S. Department of Energy under Contract No. 31256.

References

[1] A. Berres, B. Bass, J. R. New, P. Im, M. Urban, and J. Sanyal. Generating traffic-based building occupancy schedules in chattanooga, tennessee from a grid of traffic sensors. In *Proceedings of IBPSA Building Simulations 2021*, pp. 3616 – 3623, 2022. doi: 10.26868/25222708.2021.30744 1

[2] A. Berres, P. Im, K. Kurte, M. Allen-Dumas, G. Thakur, and J. Sanyal. A mobility-driven approach to modeling building energy. In *2019 IEEE International Conference on Big Data (Big Data)*, pp. 3887–3895, 12 2019. doi: 10.1109/BigData47090.2019.9006308 1

[3] J. Bezanson, A. Edelman, S. Karpinski, and V. B. Shah. Julia: A fresh approach to numerical computing. *SIAM Review*, 59(1):65–98, 2017. doi: 10.1137/141000671 2

[4] C. Brelsford, S. Tennille, A. Myers, S. Chinthavali, V. Tansakul, M. Denman, M. Coletti, J. Grant, S. Lee, K. Allen, et al. A dataset of recorded electricity outages by united states county 2014–2022. *Scientific Data*, 11(1):271, 2024. 2

[5] City of Austin. Year in review: Winter storm uri. https://data.austintexas.gov/stories/s/Year-in-Review-Winter-Storm-Uri/hpvi-b8ze/, Dec. 2021. Online; accessed: 2024-06-26. 4

[6] S. Danisch and J. Krumbiegel. Makie.jl: Flexible high-performance data visualization for Julia. *Journal of Open Source Software*, 6(65):3349, 2021. doi: 10.21105/joss.03349 2

[7] V. Do, H. McBrien, N. M. Flores, A. J. Northrop, J. Schlegelmilch, M. V. Kiang, and J. A. Casey. Spatiotemporal distribution of power outages with climate events and social vulnerability in the usa. *Nature communications*, 14(1):2470, 2023. doi: 10.1038/s41467-023-38084-6 2

[8] Z. Ebrahimpour, W. Wan, J. L. Velázquez García, O. Cervantes, and L. Hou. Analyzing social-geographic human mobility patterns using large-scale social media data. *ISPRS International Journal of Geo-Information*, 9(2), 2020. doi: 10.3390/ijgi9020125 2

[9] Federal Energy Regulatory Commission (FERC), North American Electric Reliability Corporation (NERC), Midwest Reliability Organization, Northeast Power Coordinating Council, ReliabilityFirst Corporation, SERC Corporation, Texas Reliability Entity, and Western Electricity Coordinating Council. The february 2021 cold weather outages in Texas and the South Central United States, Nov. 2021. 1

[10] Y. Feng, F. Thiemann, and M. Sester. Learning cartographic building generalization with deep convolutional neural networks. *ISPRS International Journal of Geo-Information*, 8(6), 2019. doi: 10.3390/ijgi8060258 2

[11] Z. Feng, H. Qu, S.-H. Yang, Y. Ding, and J. Song. A survey of visual analytics in urban area. *Expert Systems*, 39(9):e13065, 2022. doi: 10.1111/exsy.13065 2

[12] N. M. Flores, H. McBrien, V. Do, M. V. Kiang, J. Schlegelmilch, and J. A. Casey. The 2021 Texas power crisis: distribution, duration, and disparities. *Journal of exposure science & environmental epidemiology*, 33(1):21–31, 2023. doi: https:// 2

[13] M. C. Gonzalez, C. Hidalgo, and A.-L. Barabasi. Understanding individual human mobility patterns. *Nature*, 453:779–82, 07 2008. doi: 10.1038/nature06958 2

[14] D. Hirono, H.-Y. Wu, M. Arikawa, and S. Takahashi. Constrained optimization for disoccluding geographic landmarks in 3d urban maps. In *2013 IEEE Pacific Visualization Symposium (PacificVis)*, pp. 17–24, 2013. doi: 10.1109/PacificVis.2013.6596123 2

[15] Z. Li. *Algorithmic Foundation of Multi-Scale Spatial Representation*. CRC Press, 10 2006. doi: 10.1201/9781420008432 2

[16] Y. Liu, Z. Sui, C. Kang, and Y. Gao. Uncovering patterns of inter-urban trip and spatial interaction from social media check-in data. *PLOS ONE*, 9(1):1–11, 01 2014. doi: 10.1371/journal.pone.0086026 2

[17] L. Metzger. The Texas freeze: Timeline of events. https://environmentamerica.org/texas/center/articles/the-texas-freeze-timeline-of-events/, Jan. 2022. Online; accessed: 2024-06-26. 1

[18] Microsoft. US building footprints. https://github.com/microsoft/USBuildingFootprints, July 2024. Online; accessed: 2024-06-26. 2

[19] F. Miranda, T. Ortner, G. Moreira, M. Hosseini, M. Vuckovic, F. Biljecki, C. Silva, M. Lage, and N. Ferreira. The state of the art in visual analytics for 3d urban data. *Computer Graphics Forum*, 43, 2024. 2

[20] J. Moehl, S. Tennille, M. Denman, and A. Myers. Modelling electric utility county customers for situational awareness, 2023. 2

[21] A. Noulas, S. Scellato, R. Lambiotte, M. Pontil, and C. Mascolo. A tale of many cities: Universal patterns in human urban mobility. *PLOS ONE*, 7(5):1–10, 05 2012. doi: 10.1371/journal.pone.0037027 2

[22] B. Nsonga, A. Berres, R. Jeffers, C. Clark, H. Hagen, and G. Scheuermann. Extreme weather and the power grid: A case study of winter storm uri. In *Accepted into EnergyVis 2024: 4TH WORKSHOP ON ENERGY DATA VISUALIZATION*, 2024. 4

[23] S. K. Peterson, S. S. Clark, M. A. Shelly, and S. E. Horn. Assessing the household burdens of infrastructure disruptions in texas during winter storm uri. *Natural Hazards*, 120:7065–7104, 2024. doi: 10.1007/s11069-024-06480-w 2, 4

[24] K. Reda, A. A. Salvi, J. Gray, and M. E. Papka. Color nameability predicts inference accuracy in spatial visualizations. *Computer Graphics Forum*, 40(3):49–60, 2021. doi: 10.1111/cgf.14288 3

[25] S. Takahashi, R. Kokubun, S. Nishimura, K. Misue, and M. Arikawa. Interactive optimization for cartographic aggregation of building features. *Computer Graphics Forum*, 43(3):e15090, 2024. doi: 10.1111/cgf.15090 2

[26] V. Tansakul, A. Myers, S. Tennille, M. Denman, A. Hamaker, J. Huihui, K. Medlen, K. Allen, D. Redmon, S. Chinthavali, et al. Eagle-i power outage data 2014-2022. Technical report, Oak Ridge National Lab.(ORNL), Oak Ridge, TN (United States)., 2023. doi: 10.13139/ORNLNCCS/1975202 2

[27] Texas Department of State Health Services (DSHS). February 2021 winter storm-related deaths – Texas, Dec. 2021. 1, 4

[28] M. Yang, T. Yuan, X. Yan, T. Ai, and C. Jiang. A hybrid approach to building simplification with an evaluator from a backpropagation neural network. *International Journal of Geographical Information Science*, 36(2):280–309, 2022. doi: 10.1080/13658816.2021.1873998 2

[29] Y. Zheng, W. Wu, Y. Chen, H. Qu, and L. M. Ni. Visual analytics in urban computing: An overview. *IEEE Transactions on Big Data*, 2(3):276–296, 2016. doi: 10.1109/TBDATA.2016.2586447 2

[30] Y. A. Zheng, A. Abusafia, A. Lakhdari, S. T. T. Lui, and A. Bouguettaya. Imap: individual human mobility patterns visualizing platform. In *Proceedings of the 28th Annual International Conference on Mobile Computing And Networking*, MobiCom '22, p. 797–799. Associ-

ation for Computing Machinery, New York, NY, USA, 2022. doi: 10.1145/3495243.3558759 2

[31] Y. A. Zheng, A. Abusafia, A. Lakhdari, S. T. T. Lui, and A. Bouguettaya. Imap: individual human mobility patterns visualizing platform. In *Proceedings of the 28th Annual International Conference on Mobile Computing And Networking*, MobiCom '22, p. 797–799. Association for Computing Machinery, New York, NY, USA, 2022. doi: 10.1145/3495243.3558759 2